Letter

Ultrafast modification of the electronic structure of a correlated insulator

O. Grånäs,[1,*] I. Vaskivskyi,[1,2] X. Wang,[1] P. Thunström,[1] S. Ghimire,[3] R. Knut,[1] J. Söderström,[1] L. Kjellsson,[1] D. Turenne,[1] R. Y. Engel,[4] M. Beye,[4] J. Lu,[3] D. J. Higley,[5] A. H. Reid,[5] W. Schlotter,[5] G. Coslovich,[5] M. Hoffmann,[5] G. Kolesov,[6] C. Schüßler-Langeheine,[7] A. Styervoyedov,[8] N. Tancogne-Dejean,[9] M. A. Sentef,[9] D. A. Reis,[3] A. Rubio,[9,10] S. S. P. Parkin,[8] O. Karis,[1] J.-E. Rubensson,[1] O. Eriksson,[1,11] and H. A. Dürr[1]

[1]*Department of Physics and Astronomy, Uppsala University, Regementsvägen 1, 752 37 Uppsala, Sweden*
[2]*Center for Memory and Recording Research, University of California San Diego, 9500 Gilman Drive, La Jolla, California 92093-0401, USA*
[3]*Stanford PULSE Institute, SLAC National Accelerator Laboratory, 2575 Sand Hill Road, Menlo Park, California 94025, USA*
[4]*Department of Photon Science, DESY, Notkestraße 85, D-22607 Hamburg, Germany*
[5]*SLAC National Accelerator Laboratory, 2575 Sand Hill Road, Menlo Park, California 94025, USA*
[6]*John Paulson School of Engineering and Applied Sciences, Harvard University, Cambridge, Massachusetts 02138, USA*
[7]*Helmholtz-Zentrum Berlin für Materialien und Energie GmbH, 12489 Berlin, Germany*
[8]*Max-Planck Institut für Mikrostrukturphysik, Weinberg 2, Halle, Germany*
[9]*Max Planck Institute for the Structure and Dynamics of Matter and Center for Free-Electron Laser Science, Luruper Chaussee 149, 22761 Hamburg, Germany*
[10]*Center for Computational Quantum Physics, Flatiron Institute, New York, New York 10010 USA*
[11]*School of Science and Technology, Örebro University, SE-701 82 Örebro, Sweden*

(Received 28 December 2021; revised 22 June 2022; accepted 27 June 2022; published 16 August 2022)

A nontrivial balance between Coulomb repulsion and kinematic effects determines the electronic structure of correlated electron materials. The use of electromagnetic fields strong enough to rival these native microscopic interactions allows us to study the electronic response as well as the time scales and energies involved in using quantum effects for possible applications. We use element-specific transient x-ray absorption spectroscopy and high-harmonic generation to measure the response to ultrashort off-resonant optical fields in the prototypical correlated electron insulator NiO. Surprisingly, fields of up to 0.22 V/Å lead to no detectable changes in the correlated Ni 3*d* orbitals contrary to previous predictions. A transient directional charge transfer is uncovered, a behavior that is captured by first-principles theory. Our results highlight the importance of retardation effects in electronic screening and pinpoints a key challenge in functionalizing correlated materials for ultrafast device operation.

DOI: 10.1103/PhysRevResearch.4.L032030

Strongly correlated electron materials underlie many of the most intriguing macroscopic manifestations of quantum physics [1,2]. The source of strong electron correlation in transition-metal oxides originates in the inherent competition between the effective local Coulomb repulsion between the transition-metal *d* electrons, and orbital hybridization [3]. In the most condensed model describing interacting Fermions on a lattice, the Hubbard model, these two quantities are represented by the Hubbard U, favoring localization of electrons, and the hopping parameter t, promoting band formation. Strong electromagnetic fields may upset the balance between the hopping energy scale t and the Hubbard U, potentially inducing a dramatic change in the electronic structure, offering the possibility to control the materials properties (see Sec. IIB for an extended discussion in Ref. [4]). Recent theoretical predictions state that the prototypical correlated insulator nickel oxide exhibits a dramatic change of Hubbard U in response to nonresonant ultra strong fields [5]. To corroborate this prediction, time-resolved experimental evidence probing the site and orbital response is needed. With the advent of experimental pump-probe techniques, the response of targeted degrees of freedom can be measured. Still, the ability to probe the response of both localized electrons and those with itinerant character on ultrafast time scales requires a combination of techniques, in particular in the presence of nonresonant strong electromagnetic fields.

NiO exhibits signatures of localized atomic-like states originating with the Ni 3*d* orbitals [6] as well as bandlike dispersive electronic states [7]. The localization of Ni 3*d* orbitals is a result of a large Hubbard U in relation to the hopping t. This balance originates in a weak screening of the local Coulomb interaction between 3*d* electrons by surrounding itinerant electrons in O 2*p* and Ni 4*s* states. The O 2*p* states have a fundamental impact on optical and electrical transport properties [8], which is captured by the charge-transfer energy-scale, as the energetic overlap allows electron transfer

*oscar.granas@physics.uu.se

from O $2p$ states to the localized Ni $3d$ states. This charge transfer is also relevant for the super-exchange mechanism responsible for the antiferromagnetic order between Ni atoms along the Ni-O-Ni bond direction [9]. The balance between the charge transfer energy scale, the Hubbard U and the hopping t results in a band gap of about 4 eV in the ground state.

We use off-resonant optical fields to transiently disturb the balance between the governing energy scales. The selected 0.6-eV photon energy is midway between the well-known two-magnon resonance at 0.25 eV and the onset of d-d excitations above 0.8 eV [10]. The narrow bandwidth (100-meV FWHM) of the pump pulses implies that the probability of resonant transitions is minimal. The response is analyzed through complementary experimental techniques, probing the locality of the electronic response with resonant x-ray absorption spectroscopy (XAS), while investigating the response of hybridized valence states by monitoring the emission of higher harmonics of the driving field. Aided by nonequilibrium first-principles simulations we analyze the temporal response of the electronic structure of this correlated system. This allows to disentangle time- and spatially resolved information of response to the pump with unprecedented detail. The optical field strength was varied between 0.11 and 0.22 V/Å corresponding to optical pump fluences of 30 and 120 mJ/cm^2, respectively. In this regime, multiphoton transitions as well as Zener tunneling between valence and conduction states are suppressed (see Sec. II A in Ref. [4]).

The combination of two distinctively different characters of valence states in NiO, bandlike and localized, raises the question about the response of the electronic structure to the off-resonant field. First, the continuum states formed by the weakly correlated electronic bands respond via the so-called dynamical Franz-Keldysh effect [11–13]. The external field modifies the states so that tails from the valence and conduction states leak into the band gap region. The altered wave-function overlap induces a dynamic modification of the hopping [$t \rightarrow \tilde{t}$, see Fig. 1(b)].

Secondly, the external field may perturb screening processes in the material, resulting in a dynamic renormalization of the Hubbard U. The interaction between localized Ni $3d$ and itinerant electrons of mainly O $2p$ electrons screens the Hubbard U from an atomic value of 20–25 eV down to 7–8 eV [14]. In this scenario, strong electromagnetic fields influence crystal field levels and ligand states, causing significant changes in screening, renormalizing the Hubbard U [$U \rightarrow \tilde{U}$, see Fig. 1(c)].

It is difficult to predict which response will dominate for a given material, in particular under conditions where electrons adjust nonadiabatically to the external field, resulting in a distorted band-structure. From a theoretical perspective, out-of-equilibrium many-body methods are only able to incorporate a few bands [15]. First-principles calculations of out-of-equilibrium dynamics suffer instead from difficulties including the effect of strong correlation. One resorts either to a time-independent effective Hubbard U, or an instantaneous adaptation, representing the two extreme cases of a time-independent or an instantaneous effect on screening [5]. Predictions based on these different techniques differ qualitatively. An instantaneous screening scenario indicates a modification of U by about 10% for optical fields up to about 0.2 V/Å [5]. We estimate the expected changes in XAS resulting from an increased hopping and modification of U, for the O K and Ni L edges, respectively. The results are displayed in Figs. 1(d) and 1(e) (see Sec. II C in Ref. [4] for details).

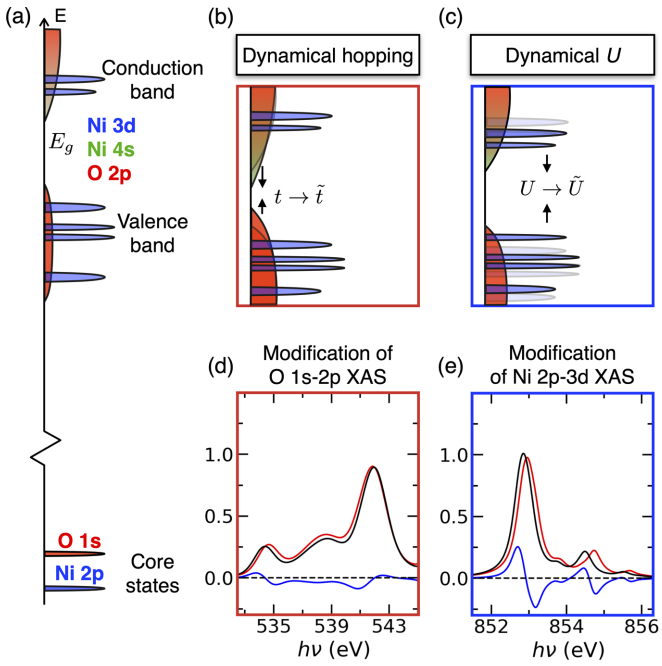

FIG. 1. (a) Schematic density of electronic states for oxygen (red) and Ni $3d$ (blue), Ni $4s$ (green) orbitals. Valence and conduction band oxygen $2p$ states show bandlike behavior whereas valence and conduction band nickel $3d$ states are split by the Coulomb repulsion between $3d$ electrons (Hubbard U). They display multiplet peaks due to their localized character. (b) Schematic illustration of expected changes of $2p$ and $3d$ states in the dynamical hopping and (c) dynamical U dominated scenarios discussed in the text. (d) Expected changes in the XAS spectra for O $1s$-$2p$ (red framed picture) modelled by adjusting the bandwidth ($t \rightarrow \tilde{t}$) and (e), Ni $2p$-$3d$ (blue framed picture) transitions modelled by changing screening ($U \rightarrow \tilde{U}$), as described in the methods section. Shown are the spectra in the ground state (red) and for the modified models representing the state driven by strong transient electric fields (black lines), as well as the differences of the two (blue lines).

We summarize the results of the pump-probe XAS experiment for the O K and Ni L edges in Fig. 2. The XAS spectra were taken at the SXR instrument of the LCLS x-ray free-electron laser in Stanford/USA. Soft x-ray probe pulses of 50-fs duration with the x-ray energy tuned to the O $1s$–$2p$ (∼535 eV photon energy) and Ni $2p$-$3d$ (∼853 eV) resonances, were incident 20° to the normal direction of ultrathin films on NiO grown epitaxially onto single-crystalline MgO(001) substrates (see Secs. I A–I C in Ref. [4]). The driving pump pulses (150-fs duration, 2-μm central wavelength) were propagating collinearly with the x rays. The pump polarization was varied during the experiment [see insets of Fig. 3(b)], while the x-ray polarization was kept fixed along the [100] NiO crystalline direction.

Figures 2(a) and 2(b) show XAS spectra taken in temporal coincidence with the pump laser pulses. It is evident that there

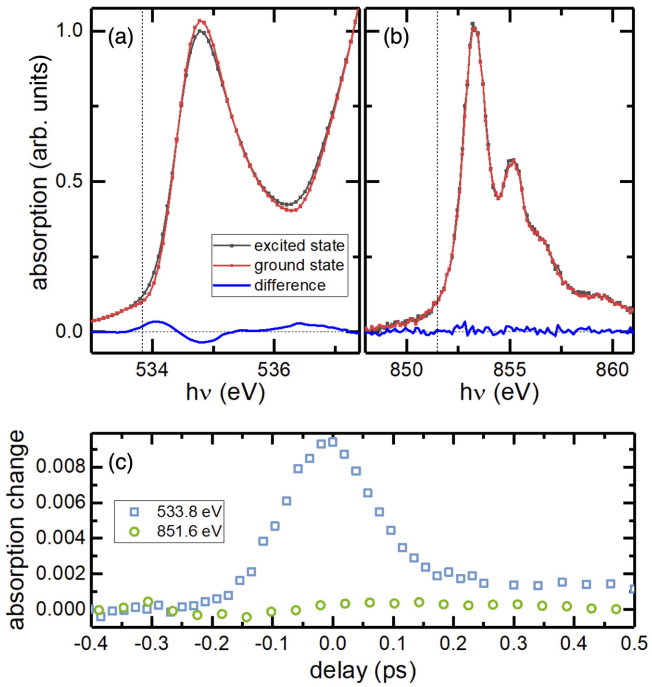

FIG. 2. (a) Measured XAS spectra for O 1s-2p transitions and (b) for Ni 2p-3d transitions. Shown are measurements with (black lines) and without (red lines) the driving laser, as well as the difference (blue lines) for the laser electric field E parallel to [100] with simultaneous arrival time of laser pump and x-ray probe. (c) Temporal evolution of the changes in O (blue squares) and Ni (green circles) XAS vs pump-probe time delay for the pre-edge, measured at 533.8-eV x-ray energy for O, while the Ni XAS was obtained for 851.6 eV [see dashed vertical line in (a) and (b)]. The peak around zero time delay of the O XAS represents the response shown in (a) and its width is essentially given by the temporal convolution of pump and probe pulses.

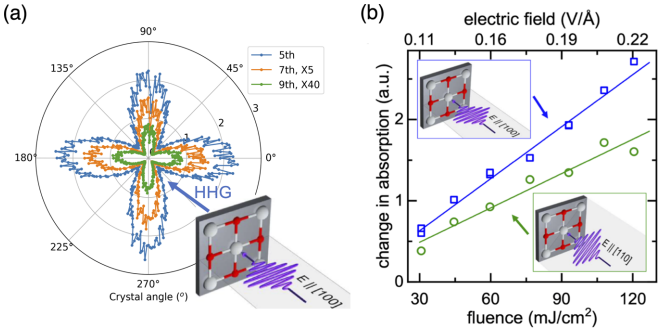

FIG. 3. (a) Measurements of the high-harmonics of the driving optical laser field vs. crystal angle relative to the [100] direction as schematically shown in the inset. The measured fifth (blue), seventh (orange), and ninth (green) harmonics show a strong preference for E || [100] directions. The width of the angular distribution decreases with increasing harmonic order. (b) Optical pump: XAS probe measurements as in Fig. 2(a) for two crystal directions as indicated in the insets. Shown are the pump-laser fluence (bottom axis) and electric peak field (top axis) dependence of the pumped-unpumped difference in O 1s-2p XAS intensity measured at an x-ray energy of 533.8 eV.

is a laser-induced modification of the O 2p conduction band [Fig. 2(a)]. However, changes of the Ni 3d-states are below the experimental detection limit [Fig. 2(b)].

The changes visible in the O 1s-2p XAS of Fig. 2(a) indicate that, when the laser-pump and x-ray-probe pulses arrive simultaneously, a spectral weight transfer takes place in the electric field modified conduction band away from the peaks observed for the ground state. This is clearly visible in the difference spectra [blue line in Fig. 2(a)] where the XAS peak intensity is attenuated while spectral weight appears at the wings of the peak both at higher and lower x-ray energies. Such a spectral broadening is reminiscent of the driving field cycle resolved dynamical Franz-Keldysh effect observed with attosecond spectroscopy in semiconductors [16]. In the dynamical Franz-Keldysh effect, characteristic changes in the band-structure are expected to be proportional to the square of the electric field, hence with a periodicity of a half-cycle of the pump [17]. We note that our experiments do not resolve the spectral changes during individual cycles of the laser driving field but rather average over the probe-pulse duration, amounting to about 12 half-cycles of the pump within the FWHM of the probe. The temporal evolution of the XAS changes versus pump-probe time delay at the absorption onset (where the changes are expected to be largest) is depicted in Fig. 2(c). Note that despite the signal being the average over many cycles, the intensity changes are significant. We also note that the changes are transient in nature, with close to zero delay at the experimental time resolution, and only about 10% of the transient remains after the pump pulse. Novelli *et al.* investigates subgap pumping of the charge-transfer compound La_2CuO_4, using a 0.95 eV photon energy for a band gap of 1.8 eV. In this compound, transient reflection reveals a substantial band-gap renormalization. Estimating the persistent changes two FHWM after the peak of the pump, about 75% of the peak change persists, whereas in our experiment only about 12% remains. The absorption in the gap region is attributed to interactions with a bosonic field in La_2CuO_4 [13], this interaction is clearly much smaller in NiO.

Electric-fields of sufficient strength may lead to high harmonic generation (HHG). The relation between the polarization direction of a linearly polarized pulse and the crystal lattice can be used to determine if multiphoton vertical transitions (governed by an anisotropic effective mass tensor) or charge-transfer dynamics (governed by the anisotropy of the real-space orbital structure) dominates the response, similar to the insulator MgO [18]. HHG is a complementary measure to the site-local probe that XAS constitutes, and measures the details of electron and hole dynamics in the hybridizing band-structure. In the scenario dominated by the dynamical hopping renormalization, electrons are accelerated along the direction of optical polarization, where an anisotropic response would indicate an anisotropy in the orbital structure. The polarization of the electronic bands leads to charge-transfer, and a transient broadening of the electronic levels via the dynamical Franz-Keldysh effect [16,19].

To address the effects of HHG generation, we study the crystal orientation dependence of HHG from monocrystalline NiO samples that are subjected to driving optical laser fields (see Sec. I D [4]). Results are shown in Fig. 3(a). The measurements show maxima along cubic directions, i.e., when

the laser field is parallel to [100] direction. In fact, the signal along [100] is about an order of magnitude higher than that along [110]. This behavior is consistent with a microscopic mechanism where a highly preferential charge transfer occurs in the direction of the O $2p$ - Ni $3d$ bonds. The direction of the O $2p$ states at the valence band maximum is pinned by the hybridization to Ni $3d$ states. However, the absence of Ni $3d$ response in the XAS measurements indicates that the charge-transfer involves final-state orbitals of different character resulting from the nonadiabatic response of the band structure. Our simulations detailed in the following sections suggests that these states are delocalized, with substantial response in the interstitial region. Because the high-harmonic generation process is extremely nonlinear such a pronounced effect can be observed. In Fig. 3(a), it is seen that the angular widths of the harmonics decrease significantly with harmonic order, approaching only few degrees for ninth-order harmonic.

The anisotropy of the harmonic emission can not be accounted for by anisotropies in the ground-state band dispersion (see Fig. S2) and we conclude that the asymmetry of the HHG spectrum as a function of polarization must result from field-induced charge transfer. This behavior is reminiscent of that observed in the uncorrelated insulator MgO indicating a more directional charge transfer for higher order harmonics [18].

Consistent with the angular dependence observed for high harmonic generation we see that the changes in the O $1s$-$2p$ XAS are more pronounced when the pump polarization is along the [100] rather than the [110] direction [see Fig. 3(b)]. This demonstrates that the O $2p$ orbitals display a pronounced directional polarization in response to the external electric field. A rationale for this is the chemical bonding of NiO, where a direct overlap of Ni $3d$ and O $2p$ states forms Ni-O-Ni bonds in the [100] direction. The [110] direction is rotated by 45°, so that the orbital overlap between Ni $3d$ and O $2p$ states is weaker. We note that the measured change in absorption is linear in fluence, and not electric field strength, indicative of the dynamical Franz-Keldysh effect. Fitting the absorption change to fluence results in exponents of 1.06 and 1.03 for [100] and [110], respectively, leaving little room for effects of any other order, for example, changes in long-range screening, linear absorption processes or high-order photon-matter interaction.

To analyze the process in detail, we modelled the dynamical hopping renormalization response of NiO using time-dependent density functional theory, including the external optical field as a vector potential A_{Ext} (see Sec. II C [4]). The fact that the experimentally measured response of the pump pulse is strong for the O $2p$ states, whereas the Ni $3d$ states are inert to the pump, allowed us to make the simplifying assumption that U is time-independent. Figure 4 displays the results calculated for one half-cycle of a sine-wave driving field with duration and amplitude identical to the applied external field used in the experimental setup. Initially we focus on changes of the charge density at the Ni and O sites, shown in Fig. 4(a) by snapshots of the density-difference $\Delta\rho(t) = \rho(0) - \rho(t)$ at T/8 and T/4, where T is the period time of 6.9 fs. The response of the charge density indicates a transient transfer of charge, predominantly from the vicinity of the O atom to the interstitial region, according to the direction of the applied electric field. A far stronger response can be seen in the vicinity of O atoms compared to Ni, consistent with the experiments. This can be understood through the stronger localization of the Ni $3d$-, as compared to O $2p$ states. The more delocalized O $2p$ states are dominated by the kinetic energy term, which is directly modified by A_{Ext}, as opposed to the Ni $3d$ states, that are dominated by the potential term while the kinetic modification has less impact.

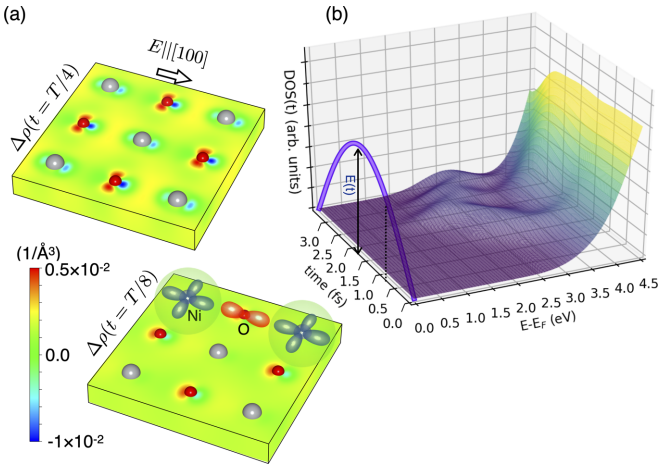

FIG. 4. (a) Calculated charge-density difference in real space as a function of time. The color represents the difference between the time-dependent and ground-state electron density, with the scale according to the color bar in units of electrons/Å^3. Yellow to red indicates an increase in electron density, and cyan to blue a decrease. Inset is a schematic of Ni s, d and O p orbitals. (b) Calculated change in the single-particle energy expectation value close to the conduction band edge, when driven with one half optical cycle of the pump, as indicated by the electric field $E(t)$ shown as blue line. The color of the electronic density of states (DOS) indicates the number of states per unit energy.

We now relate the calculated changes in electron density [Fig. 4(a)] to the measured transient XAS (Figs. 2 and 3) by calculating the time evolution of the electronic density of states (DOS) as detailed in Sec. II D. Figure 4(b) shows the DOS for energies close to the conduction band edge at times corresponding to half a cycle of A_{Ext}. At the start of the optical cycle (t = 0 fs) the DOS increases as the conduction band edge is approached above an energy of $E - E_F \approx 2.5$ eV. However, as A_{Ext} increases with time Fig. 4(b) shows that the band edge moves to significantly lower energy. There are, as an example, states all the way down to 1.5 eV at $t = 2.4$ fs. This illustrates a significant band-gap modification, expected from the dynamical Franz-Keldysh effect [16]. In addition, Fig. 4(b) demonstrates that the band-gap modulations lags behind the electric driving field. While the electric field reaches its maximum value at $t = 1.7$ fs, the in-gap states are most pronounced around 2.4 fs. This 0.7 fs delay can be attributed to the contribution of dielectric polarization currents which counteract A_{Ext} [19–21].

Experimental and theoretical results demonstrate that the response of NiO to strong subresonant electromagnetic fields is predominantly due to a transient polarization of the density, resulting in a directional charge transfer away from O to the interstitial region towards Ni. This is observed both as

a dynamical Franz-Keldysh effect in the O 1*s*-2*p* XAS and a directional strong anisotropy in high harmonic generation experiments, favoring emission when the pump is polarized along the Ni-O-Ni bond. The absence of change in Ni 2*p*-3*d* XAS shows that the charge transfer does not alter the electronic structure of 3*d* character close to the Ni core region. The agreement between our HHG and XAS results indicates that the response of NiO under the current conditions is reminiscent of that of a conventional insulator, such as MgO [18].

The apparent absence of response to the pump of the Ni L edge indicates that the screening-processes responsible for the Hubbard U is not modified on the experimental time scales considered here. This holds for accumulative effects throughout the pump duration of 150 fs, as well as for changes related to the dynamical Franz-Keldysh effect, with the relevant time scale of our pump half-cycle of 3.4 fs. Furthermore, the significant modulation of more dispersive states on a ultrashort time scale, compared to the inert screening of the Hubbard U, indicates that dispersive states respond much faster, and are more easily influenced by the optical field under the present experimental conditions. The dispersive states are the major contributor to screening of Hubbard U, hence the absence of modulation of Hubbard U must be related to the retardation of screening effects. Thus off-resonant driving fields has for NiO, and potentially for all correlated electron systems, the largest impact on dispersive, delocalized states. In this regard, the study presented here tests the speed-limit of screening of the on-site Coulomb repulsion. The results presented here indicate that nonlocal effects accommodating the screening-contribution of the itinerant states are crucial when developing theoretical and computational models for driven dynamics. In the context of low-energy Hamiltonians for many-body dynamics, these dispersive bands are projected out in the construction. How to incorporate dynamic screening originating outside the low-energy Hamiltonian is an open question.

The minute persisting signal on the O K edge indicate that little energy is pumped in to the system and the response is practically transient [see Fig. 2(c)]. The modifications of the density around the oxygen atom [see inset of Fig. 4(a)] transiently breaks the symmetry of the Ni-O-Ni bond, altering the super-exchange interaction that governs the equilibrium antiferromagnetic order in NiO [22–24]. We hypothesize that the persistent change in XAS on the O K edge is induced by excited magnetic degrees of freedom, similar to the work by Wang *et al.* where a different mechanism was used in order to stimulate a change in magnetic exchange [25]. Modifications of the magnetic exchange by subgap excitation have been observed using pump-probe methods [26]. Our measurements clearly demonstrate how the electronic structure is modified by a directional transient charge transfer along the O-Ni bond. These results, in addition to the delayed intracycle response predicted by theory, point to the importance of attosecond probes to resolve the response to the pump on intra-cycle time scales. Future measurements will be able to probe what type of possible magnetic excitation evolve on ultrafast time scales [27]. The theoretical approach described here has potential to lead the way to guide and interpret such measurements.

Note that additional details pertaining to this work can be found in Ref. [4], which includes Refs. [28–47].

O.G. acknowledge financial support from the Strategic Research Council (SSF) Grant No. ICA16-0037 and the Swedish Research Council (VR) Grant No. 2019-03901. The computations were enabled by resources provided by the Swedish National Infrastructure for Computing (SNIC), partially funded by the Swedish Research Council through Grant Agreement No. 2018-05973. O.E. acknowledges support from the Swedish Research Council (VR), the Knut and Alice Wallenberg (KAW) foundation, the Foundation for Strategic Research (SSF), the European Research Council (854843-FASTCORR), and eSSENCE. H.A.D. acknowledges support from the Swedish Research Council (VR) Grants No. 2017-06711 and No. 2018-04918. M.B. and R.Y.E. are funded by the Helmholtz Association through Grant No. VH-NG-1105. IV acknowledges support by the U.S. Department of Energy, Office of Science, Office of Basic Energy Sciences under the X-Ray Scattering Program Award No. DE-SC0017643. Operation of L.C.L.S. is supported by the U.S. Department of Energy, Office of Basic Energy Sciences under contract No. DE-AC02-76SF00515. Work at Pulse was supported by the AMOS program within the Chemical Sciences Division of the Office of Basic Energy Sciences, Office of Science, U.S. Department of Energy. S.G., J.L., and D.A.R. acknowledge the support and S.G. additionally acknowledges the Early Career Research Program. Work at CFEL was supported by the European Research Council (ERC-2015-AdG-694097), Grupos Consolidados (IT1249-19) and the Flatiron Institute, a division of the Simons Foundation. We acknowledge funding by the Deutsche Forschungsgemeinschaft (DFG) under Germany's Excellence Strategy - Cluster of Excellence Advanced Imaging of Matter (AIM) EXC 2056 - 390715994 and funding by the Deutsche Forschungsgemeinschaft (DFG). M.A.S. acknowledges funding through the Emmy Noether Programme of Deutsche Forschungsgemeinschaft (SE 2558/2-1).

[1] T. Li, A. Patz, L. Mouchliadis, J. Yan, T. A. Lograsso, I. E. Perakis, and J. Wang, Femtosecond switching of magnetism via strongly correlated spin-charge quantum excitations, Nature (London) **496**, 69 (2013).

[2] P. A. Lee, N. Nagaosa, and X.-G. Wen, Doping a Mott insulator: Physics of high-temperature superconductivity, Rev. Mod. Phys. **78**, 17 (2006).

[3] M. Imada, A. Fujimori, and Y. Tokura, Metal-insulator transitions, Rev. Mod. Phys. **70**, 1039 (1998).

[4] See Supplemental Material at http://link.aps.org/supplemental/10.1103/PhysRevResearch.4.L032030 for details on sample growth and characterization, XAS and HHG measurements and further computational details.

[5] N. Tancogne-Dejean, M. A. Sentef, and A. Rubio, Ultrafast Modification of Hubbard U in a Strongly Correlated Material: *Ab initio* High-Harmonic Generation in NiO, Phys. Rev. Lett. **121**, 097402 (2018).

[6] F. d. Groot, Multiplet effects in X-ray spectroscopy, Coordination Chem. Rev. **249**, 31 (2005).

[7] Z. X. Shen, R. S. List, D. S. Dessau, B. O. Wells, O. Jepsen, A. J. Arko, R. Barttlet, C. K. Shih, F. Parmigiani, J. C. Huang, and P. A. P. Lindberg, Electronic structure of NiO: Correlation and band effects., Phys. Rev. B **44**, 3604 (1991).

[8] G. A. Sawatzky and J. W. Allen, Magnitude and Origin of the Band Gap in NiO, Phys. Rev. Lett. **53**, 2339 (1984).

[9] D. Betto, Y. Y. Peng, S. B. Porter, G. Berti, A. Calloni, G. Ghiringhelli, and N. B. Brookes, Three-dimensional dispersion of spin waves measured in NiO by resonant inelastic x-ray scattering, Phys. Rev. B **96**, 020409(R) (2017).

[10] R. Newman and R. M. Chrenko, Optical Properties of Nickel Oxide, Phys. Rev. **114**, 1507 (1959).

[11] W. von Franz, Einfluß eines elektrischen Feldes auf eine optische Absorptionskante, Z. für Naturforschung A **13**, 484 (1958).

[12] L. V. Keldysh, Behavior of non-metallic crystals in strong electric fields, J. Exp. Tech. Phys. **33**, 994 (1958).

[13] F. Novelli, D. Fausti, F. Giusti, F. Parmigiani, and M. Hoffmann, Mixed regime of light-matter interaction revealed by phase sensitive measurements of the dynamical Franz-Keldysh effect, Sci. Rep. **3**, 1227 (2013).

[14] S. K. Panda, H. Jiang, and S. Biermann, Pressure dependence of dynamically screened Coulomb interactions in NiO: Effective Hubbard, Hund, intershell, and intersite components, Phys. Rev. B **96**, 045137 (2017).

[15] D. Golež, L. Boehnke, H. U. R. Strand, M. Eckstein, and P. Werner, Nonequilibrium GW+EDMFT: Antiscreening and Inverted Populations from Nonlocal Correlations, Phys. Rev. Lett. **118**, 246402 (2017).

[16] M. Lucchini, S. A. Sato, A. Ludwig, J. Herrmann, M. Volkov, L. Kasmi, Y. Shinohara, K. Yabana, L. Gallmann, and U. Keller, Attosecond dynamical Franz-Keldysh effect in polycrystalline diamond, Science **353**, 916 (2016).

[17] K. B. Nordstrom, K. Johnsen, S. J. Allen, A. P. Jauho, B. Birnir, J. Kono, T. Noda, H. Akiyama, and H. Sakaki, Observation of Dynamical Franz-Keldysh effect, phys. stat. sol. (b) **204**, 52 (1997).

[18] Y. S. You, D. A. Reis, and S. Ghimire, Anisotropic high-harmonic generation in bulk crystals, Nat. Phys. **13**, 345 (2017).

[19] A. Schiffrin, T. Paasch-Colberg, N. Karpowicz, V. Apalkov, D. Gerster, S. Mühlbrandt, M. Korbman, J. Reichert, M. Schultze, S. Holzner, J. V. Barth, R. Kienberger, R. Ernstorfer, V. S. Yakovlev, M. I. Stockman, and F. Krausz, Optical-field-induced current in dielectrics, Nature (London) **493**, 70 (2013).

[20] M. Schultze, E. M. Bothschafter, A. Sommer, S. Holzner, W. Schweinberger, M. Fiess, M. Hofstetter, R. Kienberger, V. Apalkov, V. S. Yakovlev, M. I. Stockman, and F. Krausz, Controlling dielectrics with the electric field of light, Nature (London) **493**, 75 (2013).

[21] S. Y. Kruchinin, F. Krausz, and V. S. Yakovlev, Colloquium: Strong-field phenomena in periodic systems, Rev. Mod. Phys. **90**, 021002 (2018).

[22] H. A. Kramers, L'interaction Entre les Atomes Magnétogènes dans un Cristal Paramagnétique, Physica **1**, 182 (1934).

[23] P. W. Anderson, Antiferromagnetism. Theory of Superexchange Interaction, Phys. Rev. **79**, 350 (1950).

[24] J. B. Goodenough, Theory of the Role of Covalence in the Perovskite-Type Manganites, Phys. Rev. **100**, 564 (1955).

[25] X. Wang, R. Y. Engel, I. Vaskivskyi, D. Turenne, V. Shokeen, A. Yaroslavtsev, O. Grånäs, R. Knut, J. O. Schunck, S. Dziarzhytski, G. Brenner, R. P. Wang, M. Kuhlmann, F. Kuschewski, W. Bronsch, C. Schüßler-Langeheine, A. Styervoyedov, S. S. P. Parkin, F. Parmigiani, O. Eriksson, M. Beye and H. A. Dürr, Ultrafast manipulation of the NiO antiferromagnetic order via sub-gap optical excitation, Faraday Discuss. (2022), doi: 10.1039/D2FD00005A.

[26] A. Kirilyuk, A. V. Kimel, and T. Rasing, Ultrafast optical manipulation of magnetic order, Rev. Mod. Phys. **82**, 2731 (2010).

[27] E. Iacocca, T. M. Liu, A. H. Reid, Z. Fu, S. Ruta, P. W. Granitzka, E. Jal, S. Bonetti, A. X. Gray, C. E. Graves, R. Kukreja, Z. Chen, D. J. Higley, T. Chase, L. Guyader, K. Hirsch, H. Ohldag, W. F. Schlotter, G. L. Dakovski, G. Coslovich, et al., Spin-current-mediated rapid magnon localisation and coalescence after ultrafast optical pumping of ferrimagnetic alloys, Nat. Commun. **10**, 1756 (2019).

[28] T. Tsuboi and W. Kleemann, Fine structure of near infrared optical absorption in NiO, J. Phys.: Condens. Matter **6**, 8625 (1994).

[29] V. I. Sokolov, V. A. Pustovarov, V. N. Churmanov, V. Y. Ivanov, N. B. Gruzdev, P. S. Sokolov, A. N. Baranov, and A. S. Moskvin, Unusual x-ray excited luminescence spectra of NiO suggest self-trapping of the d-d charge-transfer exciton, Phys. Rev. B **86**, 115128 (2012).

[30] G. R. Rossman, R. D. Shannon, and R. K. Waring, Origin of the yellow color of complex nickel oxides, J. Solid State Chem. **39**, 277 (1981).

[31] M. El-Nahass, M. Emam-Ismail, and M. El-Hagary, Structural, optical and dispersion energy parameters of nickel oxide nanocrystalline thin films prepared by electron beam deposition technique, J. Alloys Compd. **646**, 937 (2015).

[32] D. I. Khomskii, *Transition Metal Compounds* (Cambridge University Press, 2014).

[33] M. T. Hutchings and E. J. Samuelsen, Measurement of spin-wave dispersion in NiO by inelastic neutron scattering and its relation to magnetic properties, Phys. Rev. B **6**, 3447 (1972).

[34] L. A. Agapito, S. Curtarolo, and M. Buongiorno Nardelli, Reformulation of DFT + U as a Pseudohybrid Hubbard Density Functional for Accelerated Materials Discovery, Phys. Rev. X **5**, 011006 (2015).

[35] J. P. Perdew, K. Burke, and M. Ernzerhof, Generalized Gradient Approximation Made Simple, Phys. Rev. Lett. **77**, 3865 (1996).

[36] J. Lüder, J. Schött, B. Brena, M. W. Haverkort, P. Thunström, O. Eriksson, B. Sanyal, I. Di Marco, and Y. O. Kvashnin, Theory of L-edge spectroscopy of strongly correlated systems, Phys. Rev. B **96**, 245131 (2017).

[37] W. L. Roth, Magnetic structures of MnO, FeO, CoO, and NiO, Phys. Rev. **110**, 1333 (1958).

[38] M. W. Haverkort, M. Zwierzycki, and O. K. Andersen, Multiplet ligand-field theory using Wannier orbitals, Phys. Rev. B **85**, 165113 (2012).

[39] J. M. Wills, O. Eriksson, P. Andersson, A. Delin, O. Grechnyev, and M. Alouani, *Full-Potential Electronic Structure Method, Energy and Force Calculations with Density Functional and Dynamical Mean Field Theory*, Energy and Force Calculations with Density Functional and Dynamical Mean Field Theory Vol. 167 (Springer Berlin Heidelberg, Berlin, Heidelberg, 2010).

[40] J. K. Dewhurst, S. Sharma, L. Nordström, F. Cricchio, O. Grånäs, and E. K. U. Gross, The Elk Code Manual (2020).

[41] J. M. Soler, E. Artacho, J. D. Gale, A. García, J. Junquera, P. Ordejón, and D. Sánchez-Portal, The SIESTA method for

ab initio order-N materials simulation, J. Phys.: Condens. Matter **14**, 2745 (2002).

[42] G. Kolesov, O. Grånäs, R. Hoyt, D. Vinichenko, and E. Kaxiras, Real-Time TD-DFT with Classical Ion Dynamics: Methodology and Applications, J. Chem. Theory Comput. **12**, 466 (2016).

[43] G. F. Bertsch, J. I. Iwata, A. Rubio, and K. Yabana, Real-space, real-time method for the dielectric function, Phys. Rev. B **62**, 7998 (2000).

[44] S. L. Dudarev, G. A. Botton, S. Y. Savrasov, C. Humphreys, and A. P. Sutton, Electron-energy-loss spectra and the structural stability of nickel oxide: An LSDA+U study, Phys. Rev. B **57**, 1505 (1998).

[45] N. Tancogne-Dejean, M. A. Sentef, and A. Rubio, Ultrafast Transient Absorption Spectroscopy of the Charge-Transfer Insulator NiO: Beyond the Dynamical Franz-Keldysh Effect, Phys. Rev. B **102**, 115106 (2020).

[46] K. Momma and F. Izumi, VESTA: A three-dimensional visualization system for electronic and structural analysis, J Appl Crystallogr **41**, 653 (2008).

[47] J. D. Hunter, Matplotlib: A 2D Graphics Environment, Comput. Sci. Eng. **9**, 90 (2007).